ChemPubSoc Europe

DOI: 10.1002/chem.201500406

CHEMISTRY A European Journal Full Paper

Microporous Materials

Highly Luminescent Microporous Organic Polymer with Lewis Acidic Boron Sites on the Pore Surface: Ratiometric Sensing and Capture of F^- Ions

Venkata M. Suresh,[a] Arkamita Bandyopadhyay,[b] Syamantak Roy,[a] Swapan K. Pati,[c] and Tapas Kumar Maji*[a]

Abstract: Reversible and selective capture/detection of F^- ions in water is of the utmost importance, as excess intake leads to adverse effects on human health. Highly robust Lewis acidic luminescent porous organic materials have potential for efficient sequestration and detection of F^- ions. Herein, the rational design and synthesis of a boron-based, Lewis acidic microporous organic polymer (BMOP) derived from tris(4-bromo-2,3,5,6-tetramethylphenyl)boron nodes and diethynylbiphenyl linkers with a pore size of 1.08 nm for selective turn-on sensing and capture of F^- ion are reported. The presence of a vacant p_π orbital on the boron center of BMOP results in intramolecular charge transfer (ICT) from the linker to boron. BMOP shows selective turn-on blue emission for F^- ions in aqueous mixtures with a detection limit of 2.6 μM. Strong B–F interactions facilitate rapid sequestration of F^- by BMOP. The ICT emission of BMOP can be reversibly regenerated by addition of an excess of water, and the polymer can be reused several times.

Introduction

Reversible and selective detection/capture of excess F^- ions is important due to its impact on human health and the environment.[1,2] The World Health Organization recommends F^- contents in drinking water of less than 1.5 ppm, and overexposure is known to cause dental fluorosis, osteoporosis, and other serious health problems.[1] Although several methods for the detection and sequestration of F^- ions have appeared, low selectivity, poor recyclability, leaching, and weak or no analytical signal output demand the development of new materials that show both selective and reversible readout fluorescence signals and sequestration of F^- ions.[3] Recently, small-molecule sensors having vacant Lewis acidic centers have been studied for colorimetric and fluorimetric sensing of small anions such as F^- in organic solvents.[4] However, they often suffer from very low density of active sites and vulnerability to microenvironmental conditions such as solvent, and the counterion-pairing effect limits real-time monitoring of F^-.[5] On the other hand, metal complexes and small organic molecular sensors for F^- detection in solvents such as H_2O, THF, and DMF have been reported, but they suffer from poor reversibility, low recyclability, or difficulty regeneration.[6] Reversibility and easy recyclability are of the utmost importance for the commercialization and industrial application of a sensor. In this context, the confined nanospaces enclosed by a high density of F^- binding sites with fluorescence read-out signaling ability of solid porous materials[7] have potential for rapid and selective detection of F^- ions. The insoluble nature of solid porous materials facilitates heterogeneous-phase detection of F^- ions and allows easy recovery of the sensor material from aqueous solutions. Sensors based on inorganic–organic hybrid systems such as metal–organic frameworks (MOFs) have been reported, but their poor hydrolytic stability and limited regenerability due to disintegration of the framework on F^- binding limits their application.[8] In this respect, porous organic polymer solid adsorbents[9] such as conjugated microporous polymers (CMPs), pioneered by Cooper et al.,[10] have great potential for selective sensing and capture of F^- ions, owing to their strong fluorescence signaling ability and pronounced chemical/thermal and hydrolytic stability due to strong covalent linkages between their building blocks. Flexibility in design and the availability of large number of organic struts provides functionalized pore surfaces for desired applications.[11] In addition, the ability to host various guests in the confined environment of nanopores offers guest-responsive modulation of optical and electronic properties and can be exploited for sensing applications.[12] Among the CMPs,[13] heteroatom-containing conjugated porous polymers in which electron-donor atoms such as N are replaced by electron-deficient B centers have potential for the

[a] V. M. Suresh, S. Roy, Prof. Dr. T. K. Maji
Molecular Materials Laboratory
Chemistry and Physics of Materials Unit (CPMU)
Bangalore-560064 (India)
E-mail: tmaji@jncasr.ac.in

[b] A. Bandyopadhyay
New Chemistry Unit (NCU), Bangalore-560064 (India)

[c] Prof. Dr. S. K. Pati
Theoretical Sciences Unit (TSU)
Jawaharlal Nehru Centre for Advanced Scientific Research (JNCASR)
Bangalore-560064 (India)

Supporting information for this article is available on the WWW under http://dx.doi.org/10.1002/chem.201500406.

detection of F^- ions. Conjugation through the vacant p orbital on boron would introduce characteristic photophysical and electronic properties in the polymer. Therefore such a polymer would have a potential as a nonlinear optical material, as an electroluminescent and charge transporter in organic light-emitting diodes (OLEDs).[14] Herein, we report the rational design and synthesis of a boron microporous organic polymer (BMOP) containing methyl-protected triarylborane as node and diethynylbiphenyl as linker for selective and turn-on fluorescent sensing and sequestration of F^- ions with excellent recyclability from aqueous solution. High-density Lewis acidic B centers throughout the polymer facilitate selective and rapid detection of small anions, which would significantly obstruct intramolecular charge transfer (ICT) from the diethynylbiphenyl linker to the empty p_π orbital of boron. The ICT emission changes to intense blue emission on binding of F^- ion to the boron center at levels as low as 0.2 ppm in aqueous binary mixtures. Furthermore, strong covalent linkages in the polymer provide high hydrolytic stability and easy regeneration of the sensor on addition of an excess of water.

Results and Discussion

Synthesis and characterization

BMOP was synthesized by Pd^0/CuI-catalyzed Sonogashira C–C coupling between tris(4-bromo-2,3,5,6-tetramethylphenyl)boron nodes (Supporting Information, Figure S1) and 4,4′-diethynylbiphenyl linkers (Supporting Information, Figure S2), as shown in Scheme 1. The FTIR spectrum of BMOP, which shows bands at 980, 1600, and 2100 cm^{-1} corresponding to the C–B, C=C, and C≡C stretching vibrations, respectively[12a,15] (Supporting Information, Figure S3), confirmed the presence of both node and linker moieties in the polymer. Furthermore, the solid-state ^{13}C CP/MAS NMR spectrum shows a moderate signal at 90 ppm assigned to C of the C≡C bond, suggests bonding of the triarylborane node and 4,4′-diethynylbiphenyl linker (Figure 1). Other peaks ranging from 120–150 ppm can be assigned to the aromatic C atoms of phenyl rings,[12a,16] and the peak at 19 ppm to aliphatic methyl substituents of the phenyl rings.[6a,17] The presence of boron in BMOP was confirmed by X-ray photoelectron spectroscopy (XPS). The XP spectrum (Supporting Information, Figure S4), which showed a B 1s peak centered at 189.90 eV and a Br $3p_{3/2}$ peak at 184.45 eV, suggested the presence of boron and free terminal bromine of the triarylborane node in BMOP.[18] Powder XRD measurements showed a broad peak at 20° indicating amorphous nature of BMOP (Supporting Information, Figure S5).

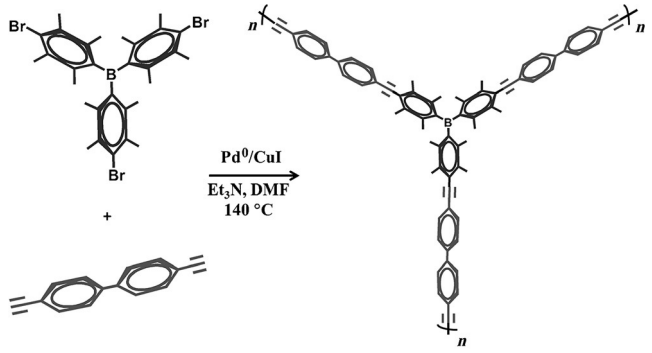

Scheme 1. Synthesis of BMOP by Sonogashira C–C coupling between tris(4-bromo-2,3,5,6-tetramethylphenyl)boron and diethynylbiphenyl.

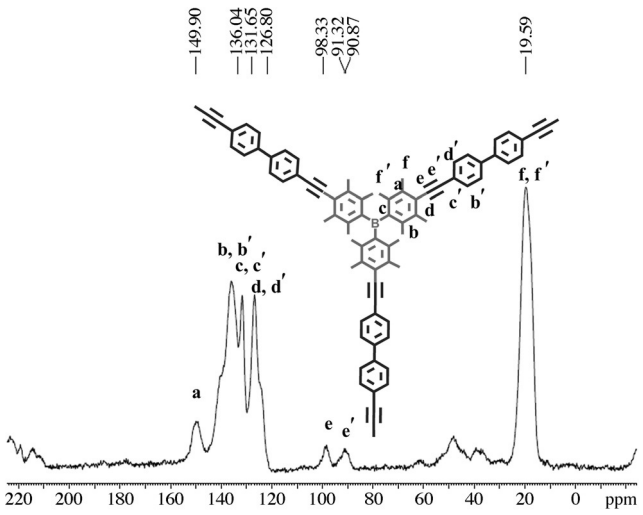

Figure 1. ^{13}C CP/MAS solid-state NMR spectrum of BMOP confirming the linkage of node and linker through a C–C bond.

SEM images showed formation of clustered spherical particles of size varying from 100 to 300 nm (Supporting Information, Figure S6). TEM images also revealed the presence of clustered particles (Supporting Information, Figure S7) and, at higher magnification, the presence of micropores in the particle (Figure 2a). Thermogravimetric analysis of BMOP showed no appreciable weight loss up to 280 °C, and further heating resulted in steady weight loss (50%) up to 720 °C (Supporting Information, Figure S8), and constant mass was observed up to 1000 °C. These results suggest the absence of any traces of $[Pd(PPh_3)_4]$ catalyst, and the remaining mass can be attributed to the presence of oxides of boron and Pd^0 nanoparticles. Such mass constancy is also observed in covalent organic frameworks and metal–organic frameworks.[19] N_2 adsorption measurements at 77 K showed a type I adsorption profile with appreciable uptake in the lower-pressure range, and the final uptake was 207 mL g^{-1} (Figure 2b). Application of the BET model to the N_2 isotherm in the range of $P/P_0 = 0.01–0.3$ yielded a surface area of 390 $m^2 g^{-1}$. A nonlocal DFT model fitted to the N_2 adsorption isotherm gave an average pore size of 1.08 nm and thus signified microporous nature of the polymer (Supporting Information, Figure S9). BMOP showed a CO_2 uptake capacity of 90 mL (18 wt%) at 195 K up to 1 atm (Figure 2b, inset) and 60 mL (12 wt%) at 273 K up to 30 bar (Supporting Information, Figure S10).

Photophysical studies

BMOP is a dark green compound in contrast to the white crystalline tris(4-bromo-2,3,5,6-tetramethyl phenyl)boron and 4,4′-diethynylbiphenyl precursors. The absorbance of BMOP is

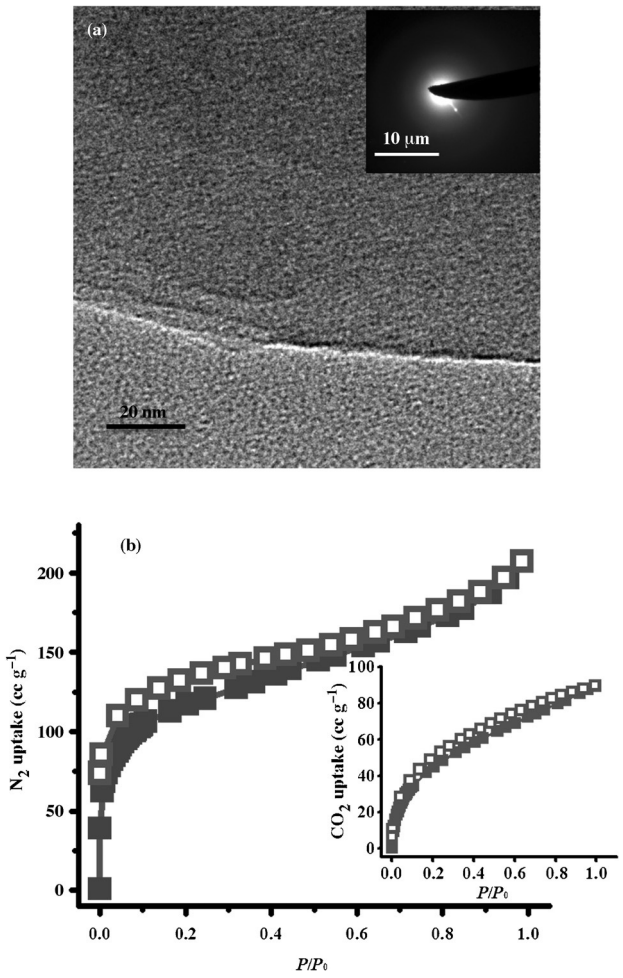

Figure 2. a) TEM image of BMOP showing micropores at higher magnification (inset: electron-diffraction pattern). b) N_2 adsorption isotherms of BMOP at 77 K (inset: CO_2 adsorption profile at 195 K).

broad and features two major UV/Vis absorption bands at 350 and 410 nm, which can be ascribed to π–π^* transition of the linker part and π–p_π(B) electron transition from the linker to the empty p orbital of boron, respectively (Supporting Information, Figure S11). In contrast to the blue emission of the linker and non-emissive behavior of tris(4-bromo-2,3,5,6-tetramethylphenyl)boron, BMOP shows strong green emission with a maximum at 520 nm (Supporting Information, Figure S11), and the excitation spectrum shows two resolved bands at 350 and 410 nm. This large redshift in emission of BMOP clearly suggests interaction between the extended linker (donor) and the boron center (acceptor) through ICT via conjugation. The ICT process was validated by solvent-dependent emission features of the polymer; in a nonpolar solvent such as hexane, BMOP shows local excited-state emission with a maximum at 410 nm originating from the extended linker, whereas in a highly polar solvent such as water the emission maximum is redshifted to 520 nm and assigned to ICT (Supporting Information, Figure S12). The dependence of the emission maxima of the polymer on solvent polarity demonstrates strong coupling between donor and acceptor in the excited state. This strong dependence of the emission maximum on solvent polarity indicates that the excited state is stabilized by polar solvents due to the high dipole moment. Furthermore, no changes in excitation spectra were observed on changing the solvent polarity, and this suggests weak coupling between donor and acceptor in the ground state (Supporting Information, Figure S13). The ICT behavior of BMOP was further studied by performing DFT calculations on the boron precursor and the smallest unit of the polymer (Figure 3a) by using the B3LYP

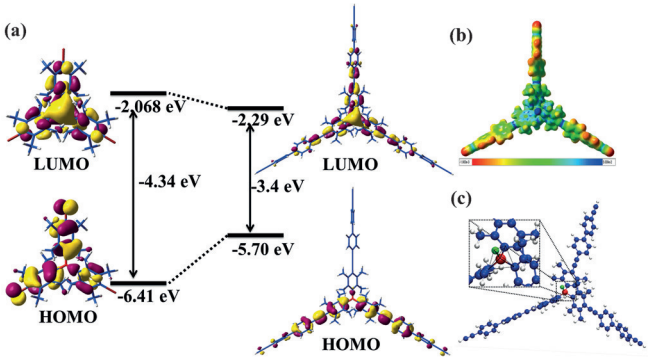

Figure 3. a) HOMO–LUMO energy level diagram of tris(2,3,5,6-tetramethyl-4-bromophenyl) boron and the smallest unit of BMOP. b) ESP plot of the smallest unit of BMOP after F^- binding (red and blue regions indicate high and low electron density, respectively). c) Energy-minimized structure of F^-@BMOP showing the changes in bonding environment around the boron center. Red: B, blue: C, green: F, silver: H.

functional and 6-31+G(d) basis set, as implemented in Gaussian 09. Molecular orbital plots of the node and smallest unit of BMOP show that HOMO and LUMO are mainly localized on the phenyl rings and boron center, respectively. TDDFT calculations suggested that the ground state and optically allowed excited state correspond to the HOMO and LUMO, respectively. This clearly suggests that ICT from the linker to the empty p_π orbital of boron occurs. The optical absorption of the smallest unit (421.2 nm, $f=1.2151$) theoretically predicted by TDDFT calculations compares fairly well with the experimental value (410 nm), and no changes in absorption maxima are observed with changing solvent polarity (Supporting Information, Figure S13). Furthermore, electrostatic potential (ESP) maps of the smallest unit of BMOP clearly reveal that the boron center is highly electron deficient (Supporting Information, Figure S14).

Fluoride sensing and capture

On the basis of the principle that boron with empty p_π orbital in BMOP would accept electrons from anions, which would perturb the ICT process and induce changes in the fluorescence signal, we studied the effect of F^- ions on the ICT emission of BMOP. No visible color change was observed in the polymer on addition of F^- ions. Initial studies were done on BMOP (5 μM) dispersed in THF, and the changes in the emission of BMOP on incremental addition of F^- in the form of tetra-*n*-butylammonium fluoride (TBAF, 13 mM) in THF were recorded. As shown in Figure S15 of the Supporting Information, the intensity of the emission band at 520 nm corresponds to

decreased ICT on addition of F^- ions, and subsequently a blue emission band appears at 420 nm and is enhanced with increasing amount of F^- ions. It is expected that, when F^- binds to boron, ICT is blocked and ICT emission decreased; however, excitation of the linker results in π^*–π emission localized on the extended linker, that is, the tetramethylphenyl-fused 1,4-diethynylbiphenyl unit. To confirm that the blue emission resulted solely from the extended linker, we calculated its excited-state optical properties. The modified extended linker shows an emission peak at 411 nm (1.9820 eV; Supporting Information, Figure S16), which is close to experimentally observed blue emission (420 nm). Also, the orbital diagram (LUMO and HOMO) confirms that this extended linker shows the characteristic π^*–π emission peak (S1→S0; Supporting Information, Figure S17), which further support the hypothesis that the strong blue emission of F^--loaded MOP (F^-@BMOP) indeed originates from the extended linker, which signifies its importance for turn-on sensing of F^- ions. The emission color of the solution changes from green to intense blue on F^- binding (Supporting Information, Figure S18). Furthermore, the ESP plot suggests that, on complexation of F^-, the boron center loses its electron-deficient character, and F^- becomes the low-electron-density species (Figure 3b and Supporting Information, Figure S19). We calculated the optimized structure for the F^--bound smallest unit (Figure 3c). The F^- ion is indeed strongly bound to the boron center by donating electrons to boron. The B–F distance of 1.47 Å in F^-@BMOP is close to that of BF_4^- (1.43 Å) and suggests strong interaction between B and F and the corresponding geometry shown in Figure 3c.

Detection of F^- in water is a challenge. The World Health Organization recommends that F^- ion content in drinking water be lower than 1.5 ppm. However, BMOP does not show significant change in emission spectra on incremental addition of fluoride ion in pure water due to high hydration enthalpy (Supporting Information, Figure S20). Hence, further experiments were carried out in aqueous/organic solvent mixtures. Initial experiments were done with BMOP (5 μM) dispersed in DMSO/H_2O (8:2) and titrated against TBAF (15 mM in DMSO/H_2O 8:2). Figure 4a shows a gradual decrease of the emission intensity at 520 nm with simultaneous increase in the blue emission intensity at 410 nm on addition of F^-. The blue emission is ascribed to π^*–π emission of the extended linker (see above). Nevertheless, the detection limit was observed to be about 20 ppm. On the other hand, THF/H_2O in (9:1) is found to be promising for detection of lower concentrations of F^- ions. As shown in Figure 4b, similar blockage of ICT emission and enhancement of blue emission from the linker was observed on incremental addition of F^- (3.5 mM) to BMOP dispersed in THF/H_2O. Strikingly, similar fluorescence response of BMOP was observed down to very low concentrations of F^-. In the Stern–Volmer plot showing the florescence response of BMOP versus equivalents of fluoride ion (THF/H_2O 9:1, initial concentration of F^-: 4.5×10^{-4} M; Supporting Information, Figure S21), the intercept or detection limit was found to be 2.6 μM. Interestingly, BMOP shows appreciable fluorescence response even at lower concentrations of F^- ions (final concentration: <2.6 μM) on soaking F^- with a dispersion of BMOP in THF/H_2O for 15 min (Supporting Information, Figure S22). This delayed fluorescence response for such low concentrations of F^- may be attributed to the longer diffusion time of F^- ion to interact with boron present in the polymer. The binding constant for F^- ion to BMOP was calculated from fluorescence titration data to be 1×10^4 M^{-1} (Supporting Information, Figure S23). It is noteworthy that BMOP is highly selective for F^- ions (Supporting Information, Figure S24) and shows no appreciable fluorescence response to other anions such as Cl^-, Br^-, I^-, NO_3^-, SO_4^{2-}, and CO_3^{2-}. This high selectivity of BMOP to F^- ions may be due to the sterically crowded binding environment created by the *ortho*-methyl groups of phenyl substituents around the boron center.[20] The most striking feature of F^- ion sensing with BMOP is its reversibility and sample recovery. Owing to the large hydration enthalpy of the F^- ion,[4b] addition of an excess of water to F^-@BMOP, regenerates the as-synthesized polymer with complete restoration of green emission, and it can recovered by simple centrifugation (Supporting Information, Figure S25).

To study the capability of BMOP in the sequestration of F^-, we carried out ^{19}F NMR spectroscopy on a solution of TBAF in which BMOP was soaked (the insoluble nature of BMOP prevented our studying of ^{11}B NMR spectral changes). A solution of TBAF/[D_6]DMSO (5 mM) was added to BMOP (0.1 mg), the mixture allowed to stand for 60 s, and BMOP removed by centrifugation. The clear solution thus obtained was analyzed for free F^- ions by ^{19}F NMR spectroscopy (Figure 5). As expected, the signal intensity of free F^- in solution decreased drastically within 60 s, and soaking for a further 60 s resulted in complete loss of the F signal in the NMR spectrum. This clearly suggests that the F^- ion is indeed captured within the porous polymer, and its coordination to a boron center is evident from the blue emission of BMOP under UV light (Figure 5, inset). Furthermore, ^1H NMR spectra of the filtrate at different intervals did not show any peaks related to integral parts of the polymer and thus clearly suggested no disintegration of the polymer on F^- ion binding (Supporting Information, Figures S26 and S27). To further prove the capture of F^- by the polymer, we carried out elemental mapping of the F^-@BMOP powder isolated by the centrifugation of the [D_6]DMSO dispersion. Elemental

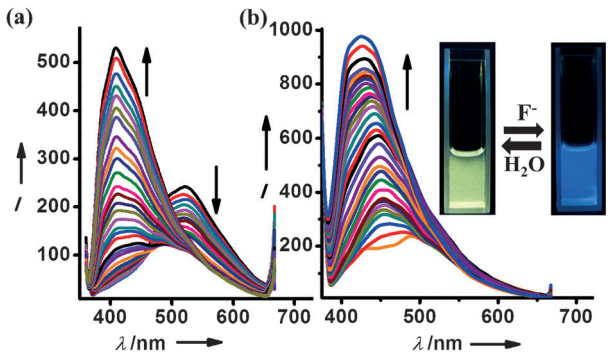

Figure 4. Changes in fluorescence spectra of BMOP on incremental addition of F^- ion in a) DMSO/H_2O (8:2) and b) THF/H_2O (9:1). Inset: images of BMOP dispersed in THF/H_2O under UV light before and after F^- addition and reversibility of the color change.

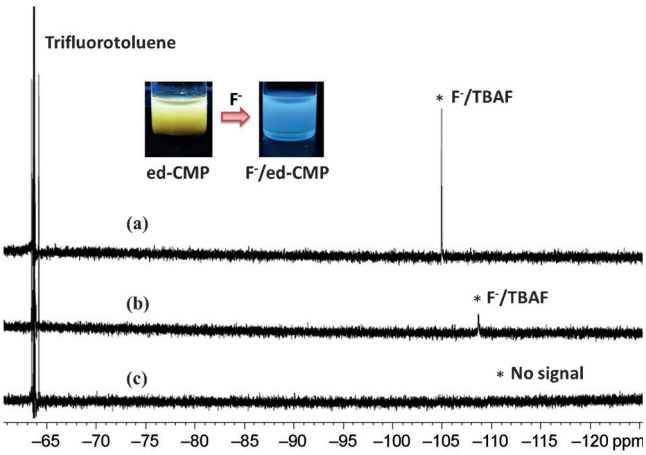

Figure 5. ^{19}F NMR spectra of 5 mM TBAF solution in [D_6]DMSO a) before, b) after 60 s, and c) after 120 s of soaking with BMOP (trifluorotoluene as standard). Inset: Change of emission color of BMOP dispersion to blue after 120 s under a UV lamp.

mapping showed a uniform distribution of F^- throughout the polymer matrix, which confirms that the F^- ion is indeed captured by BMOP through strong anion–boron interactions in the micropores of the polymer (Figure 6). These results clearly

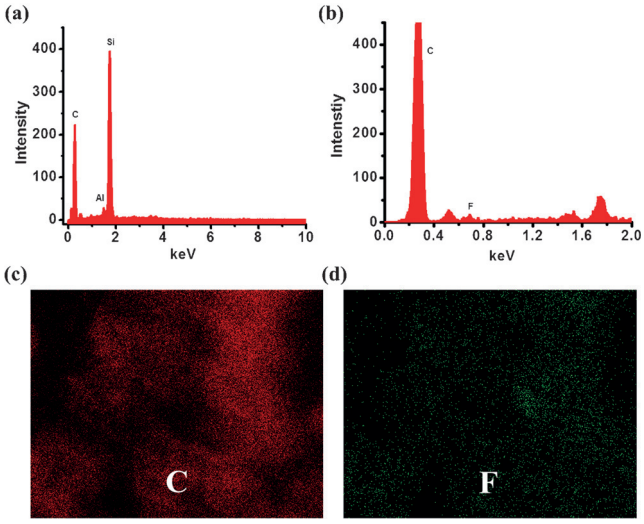

Figure 6. Energy-dispersive X-ray analysis of a) BMOP and b) F^-@BMOP, showing the presence of F^- ions in the polymer. Elemental mapping of F^-@BMOP for c) C and d) F^-, showing the presence of carbon and fluoride ion, respectively, throughout the polymer matrix.

suggest that BMOP can not only recognize but also capture F^- ions. This selective recognition and capture or sequestration of F^- ions in a π-conjugated porous polymer is unprecedented, and the detection limits are low in comparison to discrete compounds and porous scaffolds.[21] We further tested the capability of BMOP to indicate the F^- ions present in Colgate anticavity toothpaste by extracting it with THF/H_2O. As seen in Figure S28 of the Supporting Information, with incremental addition of extract solution, clear enhancement of the blue emission was observed.

Conclusion

We have demonstrated the rational design and synthesis of a Lewis acidic microporous organic polymer with high density of functional boron centers as recognition sites for selective detection of F^-. The extended conjugation of the linker through duryl groups facilitated turn-on fluorescent sensing of F^- ion by the obstruction of ICT. BMOP shows a low detection limit, and strong boron–fluoride interactions allowed facile sequestration of F^- ion. We further believe that BMOP with strong ICT emission could find applications in OLEDs and in sequestration of CO_2 through Lewis acid–base interactions with boron.

Acknowledgements

We thank Prof. C. N. R. Rao for his support and encouragement, Mrs. Usha for TEM measurements, and NMR research centre IISc, Bangalore, for solid-state ^{13}C NMR measurements. V.M.S. and S.R. thank CSIR and DST for fellowship and funding, T.K.M. thanks DST, Government of India for financial support.

Keywords: boron · Lewis acids · microporous materials · polymers · sensors

[1] a) J. Fawell, K. Bailey, J. Chilton, E. Dahi, L. Fewtrell, Y. MagaraWorld Health Organization (WHO). *Fluoride in Drinking Water*, IWA Publishing, London, **2006**.

[2] a) P. Adler, *Fluorides and Health*, World Health Organization, Geneva, **1970**; b) E.W. Rice, R. B. Baird, A. D. Eaton, L. S. Clesceri, *Standard Methods for the Examination of Water and Wastewater*, American Public Health Association, American Water Works Association, Water Environment Federation, **1998**.

[3] a) S. Jagtap, M. K. Yenkie, N. Labhsetwar, S. Rayalu, *Chem. Rev.* **2012**, *112*, 2454 – 2466; b) B. Pan, J. Xu, B. Wu, Z. Li, X. Liu, *Environ. Sci. Technol.* **2013**, *47*, 9347 – 9354.

[4] a) Z. M. Hudson, S. Wang, *Acc. Chem. Res.* **2009**, *42*, 1584 – 1596; b) C. R. Wade, A. E. J. Broomsgrove, S. Aldridge, F. P. Gabbaï, *Chem. Rev.* **2010**, *110*, 3958 – 3984.

[5] E. Galbraith, T. D. James, *Chem. Soc. Rev.* **2010**, *39*, 3831 – 3842.

[6] a) T. Liu, A. Nonat, M. Beyler, M. Regueiro-Figueroa, K. Nchimi Nono, O. Jeannin, F. Camerel, F. Debaene, S. Cianférani-Sanglier, R. Tripier, C. Platas-Iglesias, L. J. Charbonnière, *Angew. Chem. Int. Ed.* **2014**, *53*, 7259 – 7263; *Angew. Chem.* **2014**, *126*, 7387 – 7391; b) S. Guha, S. Saha, *J. Am. Chem. Soc.* **2010**, *132*, 17674 – 17677; c) X. Y. Liu, D. R. Bai, S. Wang, *Angew. Chem. Int. Ed.* **2006**, *45*, 5475 – 5478; *Angew. Chem.* **2006**, *118*, 5601 – 5604; d) P. Bose, P. Ghosh, *Chem. Commun.* **2010**, *46*, 2962 – 2964; e) R. Hu, J. Feng, D. Hu, S. Wang, S. Li, Y. Li, G. Yang, *Angew. Chem. Int. Ed.* **2010**, *49*, 4915 – 4918; *Angew. Chem.* **2010**, *122*, 5035 – 5038.

[7] a) M. D. Allendorf, C. A. Bauer, R. K. Bhakta, R. J. T. Houk, *Chem. Soc. Rev.* **2009**, *38*, 1330 – 1352; b) L. E. Kreno, K. Leong, O. K. Farha, M. Allendorf, R. P. Van Duyne, J. T. Hupp, *Chem. Rev.* **2012**, *112*, 1105 – 1125; c) S. Fischer, J. Schmidt, P. Strauch, A. Thomas, *Angew. Chem. Int. Ed.* **2013**, *52*, 12174 – 12178; *Angew. Chem.* **2013**, *125*, 12396 – 12400; d) X. Liu, Y. Xu, D. Jiang, *J. Am. Chem. Soc.* **2012**, *134*, 8738 – 8741; e) Y. Cui, Y. Yue, G. Qian, B. Chen, *Chem. Rev.* **2012**, *112*, 1126 – 1162.

[8] a) F. M. Hinterholzinger, B. Rühle, S. Wuttke, K. Karaghiosoff, T. Bein, *Sci. Rep.* **2013**, *3*, 2562; b) S. Saha, B. Akhuli, I. Ravikumar, P. S. Lakshminarayanan, P. Ghosh, *CrystEngComm* **2014**, *16*, 4796 – 4804.

[9] a) R. Dawson, E. Stoeckel, J. R. Holst, D. J. Adams, A. I. Cooper, *Energy Environ. Sci.* **2011**, *4*, 4239 – 4245; b) A. I. Cooper, *Adv. Mater.* **2009**, *21*, 1291 – 1295; c) H. A. Patel, F. Karadas, J. Byun, J. Park, E. Deniz, A. Canlier, Y. Jung, M. Atilhan, C. T. Yavuz, *Adv. Funct. Mater.* **2013**, *23*, 2270 – 2276;

d) S. Hug, M. E. Tauchert, S. Li, U. E. Pachmayr, B. V. Lotsch, *J. Mater. Chem.* **2012**, *22*, 13956 – 13964.

[10] J. X. Jiang, F. Su, A. Trewin, C. D. Wood, N. L. Campberll, H. Niu, C. Dickinson, A. Y. Ganin, M. J. Rosseinsky, Y. Z. Khimyak, A. I. Cooper, *Angew. Chem. Int. Ed.* **2008**, *47*, 2458 – 2462; *Angew. Chem.* **2008**, *120*, 2492 – 2496.

[11] a) Z. Chang, D.-S. Zhang, Q. Chen, X. H. Bu, *Phys. Chem. Chem. Phys.* **2013**, *15*, 5430 – 5442; b) A. Thomas, *Angew. Chem. Int. Ed.* **2010**, *49*, 8328 – 8344; *Angew. Chem.* **2010**, *122*, 8506 – 8523; c) H. A. Patel, S. H. Je, J. Park, D. P. Chen, Y. Jung, C. T. Yavuz, A. Coskun, *Nat. Commun.* **2013**, *4*, 1357; d) K. V. Rao, S. Mohapatra, C. Kulkarni, T. K. Maji, S. J. George, *J. Mater. Chem.* **2011**, *21*, 12958 – 12963; e) K. V. Rao, R. Haldar, T. K. Maji, S. J. George, *Chem. Mater.* **2012**, *24*, 969 – 971.

[12] a) V. M. Suresh, S. Bonakala, S. Roy, S. Balasubramanian, T. K. Maji, *J. Phys. Chem. C* **2014**, *118*, 24369 – 24376; b) K. V. Rao, S. Mohapatra, T. K. Maji, S. J. George, *Chem. Eur. J.* **2012**, *18*, 4505 – 4509; c) J.-X. Jiang, A. Trewin, D. J. Adams, A. I. Cooper, *Chem. Sci.* **2011**, *2*, 1777 – 1781; d) L. Chen, Y. Honsho, S. Seki, D. Jiang, *J. Am. Chem. Soc.* **2010**, *132*, 6742 – 6748; e) S. Ren, R. Dawson, D. J. Adams, A. Cooper, *Polym. Chem.* **2013**, *4*, 5585 – 5590.

[13] a) G. Cheng, T. Hasell, A. Trewin, D. J. Adams, A. I. Cooper, *Angew. Chem. Int. Ed.* **2012**, *51*, 12727 – 12731; *Angew. Chem.* **2012**, *124*, 12899 – 12903; b) J. Brandt, J. Schmidt, A. Thomas, J. D. Epping, J. Weber, *Polym. Chem.* **2011**, *2*, 1950 – 1952.

[14] a) N. Matsumi, Y. Chujo, *Polym. J.* **2007**, *40*, 77 – 89; b) W.-M. Wan, F. Cheng, F. Jäkle, *Angew. Chem. Int. Ed.* **2014**, *53*, 1 – 6; *Angew. Chem.* **2014**, *126*, 1 – 1; c) P. Chen, F. Jäkle, *J. Am. Chem. Soc.* **2011**, *133*, 20142 – 20145; d) F. Jäkle, *Chem. Rev.* **2010**, *110*, 3985 – 4022.

[15] a) A. P. Cote, A. I. Benin, N. W. Ockwig, M. O'Keeffe, A. J. Matzger, O. M. Yaghi, *Science* **2005**, *310*, 1166 – 1170; b) R. Dawson, A. Laybourn, Y. Z. Khimyak, D. J. Adams, A. I. Cooper, *Macromolecules* **2010**, *43*, 8524 – 8530.

[16] a) J.-X. Jiang, F. Su, A. Trewin, C. D. Wood, H. Niu, J. T. A. Jones, Y. Z. Khimyak, A. I. Cooper, *J. Am. Chem. Soc.* **2008**, *130*, 7710 – 7720; b) J.-X. Jiang, A. Trewin, F. Su, C. D. Wood, H. Niu, J. T. A. Jones, Y. Z. Khimyak, A. I. Cooper, *Macromolecules* **2009**, *42*, 2658 – 2666.

[17] B. S. Ghanem, M. Hashem, K. D. M. Harris, K. J. Msayib, M. Xu, P. M. Budd, N. Chaukura, D. Book, S. Tedds, A. Walton, N. B. McKeown, *Macromolecules* **2010**, *43*, 5287 – 5294.

[18] a) C. Ronning, D. Schwen, S. Eyhusen, U. Vetter, H. Hofsäss, *Surf. Coat. Technol.* **2002**, *158*, 382 – 387; b) L. Ci, L. Song, C. Jin, D. Jariwala, D. Wu, Y. Li, A. Srivastava, Z. F. Wang, K. Storr, L. Balicas, F. Liu, P. M. Ajayan, *Nat. Mater.* **2010**, *9*, 430 – 435; c) A. F. Lee, Z. Chang, S. F. J. Hackett, A. D. Newman, K. Wilson, *J. Phys. Chem. C* **2007**, *111*, 10455 – 10460.

[19] a) G. M. Scheuermann, L. Rumi, P. Steurer, W. Bannwarth, R. Muelhaupt, *J. Am. Chem. Soc.* **2009**, *131*, 8262 – 8270; b) S. Mandal, D. Roy, R. V. Chaudhari, M. Sastry, *Chem. Mater.* **2004**, *16*, 3714 – 3724; c) L. Lin, T. Zhang, X. Zhang, H. Liu, K. L. Yeung, J. Qiu, *Ind. Eng. Chem. Res.* **2014**, *53*, 10906 – 10913; d) E. L. Spitler, B. T. Koo, J. L. Novotney, J. W. Colson, F. J. Uribe-Romo, G. D. Gutierrez, P. Clancy, W. R. Dichtel, *J. Am. Chem. Soc.* **2011**, *133*, 19416 – 19421.

[20] a) S. Solé, F. P. Gabbai, *Chem. Commun.* **2004**, 1284 – 1285; b) M. Melaimi, F. P. Gabbai, *J. Am. Chem. Soc.* **2005**, *127*, 9680 – 9681.

[21] a) N. N. Adarsh, A. Grélard, E. J. Dufourc, P. Dastidar, *Cryst. Growth Des.* **2012**, *12*, 3369 – 3373; b) B. Chen, L. Wang, F. Zapata, G. Qian, E. B. Lobkovsky, *J. Am. Chem. Soc.* **2008**, *130*, 6718 – 6719.

Received: January 31, 2015
Published online on June 12, 2015

